

A Web Portal for the Management, Visualization, and Quality Control of Mobile LiDAR/Image Data along Transportation Corridors

Sang-Yeop Shin, Mona Hodaei, Aser Eissa, Youssef Hany, Jidong Liu, Sungwoong Hyung, Sangyoon Park, Raja Manish, and Ayman Habib

Lyles School of Civil and Construction Engineering, Purdue University, West Lafayette, USA -
(shin337, mhodaei, eissaa, yaboelma, liu2845, hyungs, park1858, rmanish, ahabib)@purdue.edu

Keywords: Mobile Mapping Systems, Web Portal Visualization, LiDAR, Transportation Corridors, Quality Control

Abstract

Efficient management of transportation corridors depends on the availability and effective analysis of high-quality geospatial data. Recent advancements have focused on Mobile Mapping Systems (MMS), which integrate Global Navigation Satellite System/Inertial Navigation System (GNSS/INS), Red-Green-Blue (RGB) cameras, and LiDAR units. However, the large volume of collected data and specialized software/hardware requirements often limit data accessibility and visualization by stakeholders. This study focuses on facilitating accessibility to transportation geospatial data by developing a Potree-based web portal for better management, visualization, and quality control of such data. The developed web portal enhances end-users' capabilities by providing primary quality control tools for assessing the georeferencing accuracy of multi-modal, multi-platform, and multi-temporal geospatial data. Users can also utilize these quality control tools to validate the calibration of Pan/Tilt/Zoom (PTZ) cameras installed along transportation corridors. Validating the calibration of PTZ cameras allows for precise pointing of these cameras to investigate the cause of traffic congestions and improve response activities by Transportation Management Centers (TMCs). Apart from the primary tools, the proposed portal also offers specialized functionalities to handle derived products from MMS data that can be used for the assessment of pavement markings condition—which is necessary for the safe operation of connected and autonomous vehicles (CAVs).

1. Introduction

Advancements in remote sensing technologies enabled the development of Mobile Mapping Systems (MMS), facilitating efficient and precise data collection along transportation corridors. Modern MMS integrate Light Detection and Ranging (LiDAR) sensors, Red-Green-Blue (RGB) cameras, and an integrated Global Navigation Satellite System/Inertial Navigation System (GNSS/INS) unit to deliver georeferenced imagery and 3D point clouds (Toth et al., 2009). Efficient road management requires the collection and analysis of various geospatial datasets, such as LiDAR point clouds and geo-tagged imagery, which provide critical information for improving roadway safety (Brinster et al., 2024). However, obtaining high-accuracy georeferenced data from MMS depends on accurate system calibration and valid trajectory information. High-quality geospatial data constitute a valuable resource for roadway network assets inventory and data-driven decision-making. Despite these benefits, many users who rely on products from MMS geospatial data—such as lane width within work zones, pavement markings condition assessment, bridge inspection, and/or drainage system evaluation—lack access to specialized hardware and software for fully utilizing such data and products (Scheiblaue et al., 2011; Schütz et al., 2019).

Traditionally, geospatial data visualization requires users to install third-party software such as CloudCompare (Girardeau-Montaut, 2016), which demands high-end hardware to manage large LiDAR datasets. Moreover, these tools are often not intuitive for efficiently visualizing and manipulating the data and derived products. To address these challenges, several web-based platforms for geospatial data visualization have been developed, including Cesium (Liu et al., 2023) and Plas.io (Plas.io., 2014). One of the most widely used open-source

WebGL-based platforms is Potree (Schütz et al., 2015; Schütz et al., 2019). Potree is specifically designed for efficient visualization of large-scale point clouds within a web browser, eliminating the need for software installation. In this study, Potree is adopted due to its following characteristics: 1) the ability of simultaneous visualization of image and point cloud data, 2) no requirement for local data storage, 3) no requirement for software installation, 4) availability of annotation tools, and 5) flexibility for customized tool development. While prior studies have utilized Potree for applications in Building Information Modeling (BIM) (Yeshwanth Kumar et al., 2019) and healthcare analytics (Carey et al., 2021), they did not consider transportation data management or quality control of geospatial data. Efficient transportation infrastructure management by agencies such as Departments of Transportation (DOTs) and Traffic Management Centers (TMCs) requires the integration of multi-modal, multi-platform, and multi-temporal geospatial data. These agencies rely on mobile LiDAR and image data to enhance traffic flow, monitor road conditions, and improve highway safety. However, the large volume and complexity of MMS image and LiDAR data/products pose significant challenges. Even though existing visualization tools can handle massive LiDAR point clouds and imagery, they often lack the necessary functionalities required by DOTs and TMCs. These agencies need solutions that go beyond visualization by incorporating tools for data-driven decision-making and transportation corridor management (Hawkins, 2013).

This study addresses the needs of transportation data management by integrating advanced functionalities for the manipulation and quality control of multi-modal, multi-platform, and multi-temporal geospatial data and derived products. Specifically, the study aims at developing a web portal for efficient storage, visualization, and manipulation of geospatial

data via an intuitive user interface. By integrating advanced functionalities for georeferencing quality assessment, the web-based platform enables end-users to interpret and analyze geospatial datasets/products. The objectives of the proposed MMS web portal are: 1) providing quality control tools for multi-modal/multi-temporal/multi-platform geospatial data to enhance the reliability of highway management decisions, and 2) equipping end-users with a range of specialized functionalities designed for analyzing MMS-derived products.

The remainder of this paper is organized as follows: Section 2 introduces the design of the MMS web portal; Section 3 presents the web portal's implementation and validation through several case studies related to transportation corridors. Finally, Section 4 provides discussion and concluding remarks.

2. Design of the MMS Web Portal

2.1 Motivation

Effective management of transportation corridors requires quality verification of multi-source, multi-modal, and multi-temporal geospatial datasets. Even though tools for refining positional accuracy of geospatial data/products do exist, non-expert users at DOTs and TMCs often lack quality control mechanisms (for example, to verify 2D/3D data alignment). Augmenting existing visualization environments with data validation tools would significantly improve their usability and effectiveness. One critical application is work zone management, where frequent roadway changes make it essential to verify the agreement between as-designed and as-built lane width values (Ravi et al., 2019; Cheng et al., 2024). Identifying and visualizing road segments with substandard lane widths is crucial to minimizing congestion and reducing back-of-queue crashes (Habib et al., 2018). Moreover, the proliferation of autonomous and connected vehicles (CAVs) and growing reliance on Driver Assistance Systems (DASS) necessitate continuous evaluation of lane markings visibility, traditionally conducted through retroreflectivity analysis (Zehr et al., 2019). Mobile LiDAR offers valuable insights into the reflectivity of lane markings through point cloud intensity data (Mahlberg et al., 2021). However, DOTs and TMCs lack specialized tools to interpret and utilize LiDAR intensity data for prioritizing lane markings maintenance activities (Cheng et al., 2020; Cheng et al., 2022). Additionally, traffic monitoring by TMCs relies on Pan/Tilt/Zoom (PTZ) cameras to assess traffic flow and diagnose congestion causes (Matthew et al., 2023; Shen et al., 2023). However, the accuracy of PTZ camera pointing depends on proper calibration, whose validity needs to be frequently checked due to environmental conditions and repeated maintenance of these cameras.

The proposed web portal aims to address the above gaps by creating an environment capable of handling multi-modal/multi-temporal/multi-platform geospatial datasets and derived products. By integrating these diverse data sources, the web portal serves as a comprehensive platform for visualization, quality assessment, and decision support, enabling DOTs and TMCs to efficiently manage transportation networks. The following subsections provide detailed description of the web portal architecture and the key functionalities designed to enhance transportation infrastructure management.

2.2 Architecture of the MMS Web Portal

The architecture of the MMS web portal, depicted in Figure 1, comprises three main components: 1) front-end, 2) back-end,

and 3) database. The front-end provides a graphical user interface (GUI) through which users can interact with the portal by issuing commands to visualize and analyze geospatial data including LiDAR point clouds and geo-tagged imagery. The back-end handles data processing by executing server-side applications that manage the geospatial data in response to user inputs from the front-end. In this study, the back-end is hosted on a Unix server as a virtual machine, with specifications detailed in Table 1. The virtual machine serves as a centralized repository with links to geospatial datasets acquired by LiDAR and imaging systems. The collected geospatial datasets, on the other hand, are stored in a 30 TB shared server. In addition to manipulating LiDAR and geo-tagged imagery data, the system provides additional functionalities that allow users to conduct the following operations: 1) conduct quality control of image and LiDAR data georeferencing through backward/forward projection functions, 2) visualize extracted lane marking point clouds, 3) inspect lane marking intensity and lane width profiles, 4) analyze intensity-retroreflectivity scatter plots to confirm the possibility of using the LiDAR intensity as a precursor to lane marking retroreflectivity, and 5) validate the calibration of PTZ cameras as a prerequisite for precise pointing. Further details related to these functionalities are provided in the following section.

2x CPU	Intel(R) Xeon(R) Gold 6248R CPU @ 3.00GHz
RAM	4 GB
Storage Space	60 GB

Table 1. Unix server's hardware specifications.

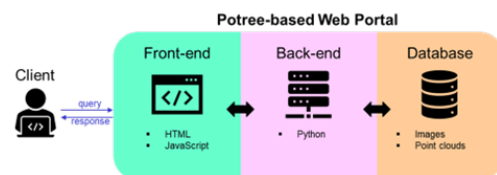


Figure 1. Illustration of the MMS web portal architecture, showing the front-end, back-end, and database.

2.3 Built-in/Developed Functionalities

The MMS web portal provides a range of built-in and developed functionalities to facilitate user-friendly interaction with geospatial data/products for informed decision-making. These features, illustrated in Figure 2, allow users to efficiently visualize, analyze, and manipulate geospatial data. As shown in Figure 3, users can upload various geospatial datasets/products, including original point clouds, bare-earth points, extracted lane markings (Figures 3a, 3b, and 3c, respectively). Figure 4 shows the web portal with a geo-tagged image imported and overlaid on the LiDAR point cloud, illustrating the georeferencing quality of the 2D imagery and 3D point cloud. In such visualizations, georeferencing artifacts will show as misalignment between corresponding image and LiDAR features – such as lane markings, utility poles, etc. For example, Figure 4a illustrates the case of well-aligned geo-tagged imagery and LiDAR point cloud, with a highlighted region to show the smooth transition of bridge features between these modalities. On the other hand, Figure 4b shows misaligned geo-tagged imagery with LiDAR data, as can be seen by the non-smooth transition of the signage boundaries between the 3D view and corresponding perspective view of the 2D image. The web portal interface also includes several built-in tools for data manipulation. For example, Figure 5 showcases the profile extraction tool for users to examine the level of detail in

extracted profiles and evaluate alignment of multi-modal/multi-platform/multi-temporal LiDAR point clouds.

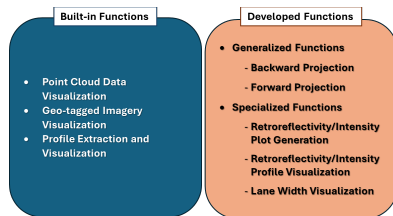


Figure 2. Illustration of built-in/developed functions integrated within the proposed web portal.

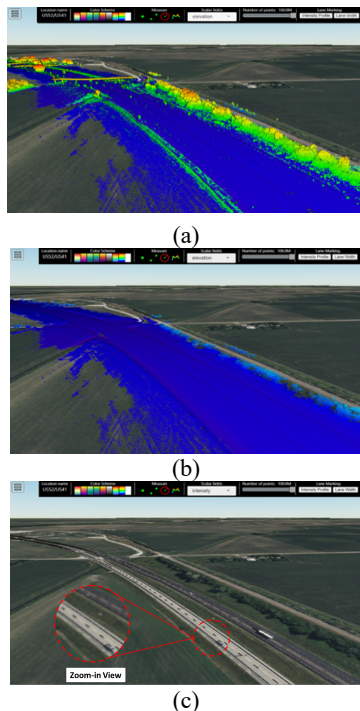


Figure 3. Illustration of web portal visualization of 3D data: (a) original point cloud colored by height, (b) bare earth point cloud colored by height, and (c) extracted lane markings point cloud colored by intensity.

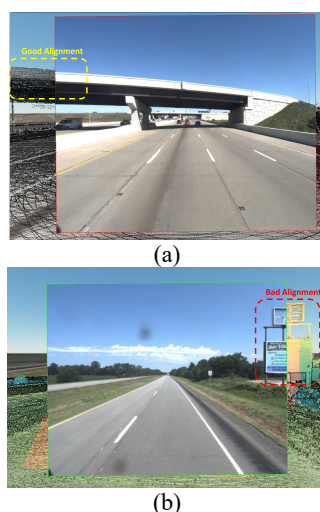


Figure 4. Illustration of web portal visualization of geo-tagged 2D imagery and 3D LiDAR data, showing: (a) well-aligned bridge features, and (b) misaligned traffic signage boundaries.

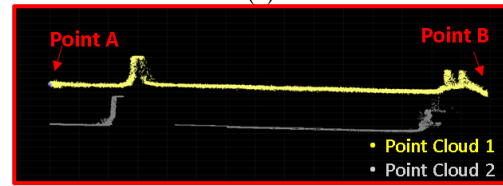
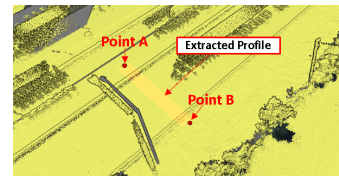


Figure 5. Illustration of (a) a profile location and (b) extracted profile highlighting the misalignment between two point clouds in yellow and grey.

In addition to the built-in tools, the web portal features several new functionalities developed in this work to enhance georeferencing data quality checks and asset management. The primary addition is the general functionalities for backward and forward projection (which are further described in Section 2.3.1) developed to assess the georeferencing/alignment quality of LiDAR data and geo-tagged imagery. Other than using these functionalities to evaluate the positional quality of 2D/3D data/products from MMS, they can be also used to validate the calibration of PTZ cameras for precise pointing applications. As stated earlier, lane marking inventory is a critical component. Therefore, functionalities for visualizing MMS-derived products such as lane markings, intensity profiles, and lane width estimates have also been developed. Specifically, these functionalities include: 1) visualization of a lane marking intensity profile along with corresponding 3D LiDAR and 2D image points for a selected query point in the intensity profile, 2) visualization of a lane width profile, along with corresponding 3D LiDAR and 2D image points for a selected query point in the lane width profile, and 3) scatter plot visualization of lane marking LiDAR intensity and standard retroreflectivity (collected by other devices), combined with corresponding 3D LiDAR and 2D image points for a selected query point in the scatter plot. Such functionalities are explained in Section 2.3.2.

2.3.1 Developed Functionalities for General Evaluation of Georeferencing Quality

The backward and forward projection functions of the web portal are used to visualize conjugate features in imagery and LiDAR data. The backward projection takes an object point from the LiDAR point cloud and back-projects it onto the 2D images where the point is visible (Figure 6a). The forward projection, on the other hand, starts by selecting a point in an image and projecting it onto the corresponding LiDAR point cloud (Figure 6b). These developed functions can be used to evaluate the georeferencing quality of 2D/3D geospatial data and derived products. For example, in the backward projection, 2D misalignment between the actual point and its backward projection can be quantified to assess the georeferencing accuracy in pixel units. This functionality could be used to validate a PTZ camera's intrinsic and extrinsic calibration parameters, essential for maintaining their effectiveness in traffic flow monitoring, traffic incident detection, and managing emergency response. The demonstration of using the developed backward/forward projection functions to facilitate PTZ camera calibration validation will be discussed further in Section 3.1.2.

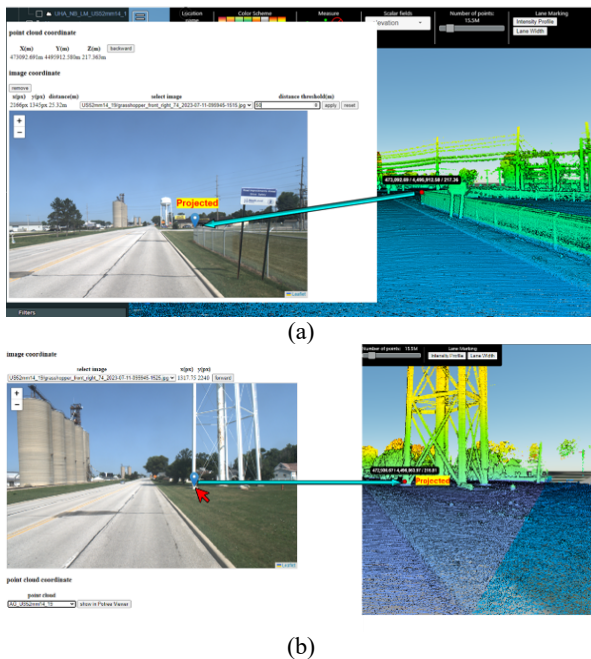


Figure 6. Illustration of (a) backward projection of an object point from the LiDAR point cloud onto a 2D image where the point is visible and (b) forward projection of a selected image point onto the corresponding LiDAR point cloud.

2.3.2 Specialized Functionalities Developed for Asset Management

Maintaining large-scale road networks requires continuous monitoring of pavement surface condition, lane markings visibility, and signage occlusions. The developed web portal includes tools for visualizing lane markings intensity profiles, along with scatter plots, if any, between LiDAR intensity and standard retroreflectivity measured by DOT/contractor dedicated devices. These visualization functions can be used as a reporting mechanism for assessing the condition of lane markings based on their intensity and retroreflectivity. Users can visualize the intensity profile and select a specific point within the profile, as demonstrated in Figure 7. In Figure 7a, the selected point is displayed on the lane marking point cloud and backward-projected onto the nearest image where it is visible. Similar to intensity profile visualization, the web portal includes a function for the visualization of a lane width profile and displaying the corresponding point-pair in the LiDAR point cloud and corresponding image for a selected location in the profile as illustrated in Figure 7b. This function provides valuable insights for identifying locations that fall below standard lane width requirements, promoting more effective communication between DOT staff and work zone contractors. Moreover, the web portal supports scatter plot visualization for intensity-retroreflectivity analysis, which is used to identify anomalies and determine whether LiDAR intensity or retroreflectivity better represents the lane marking condition, as presented in Figure 7c. An example showing regions where high intensity corresponds to low retroreflectivity and vice versa is presented in Section 3.2. By integrating these visualization and analysis tools, the web portal facilitates efficient, data-driven decision-making for roadway maintenance and safety management.

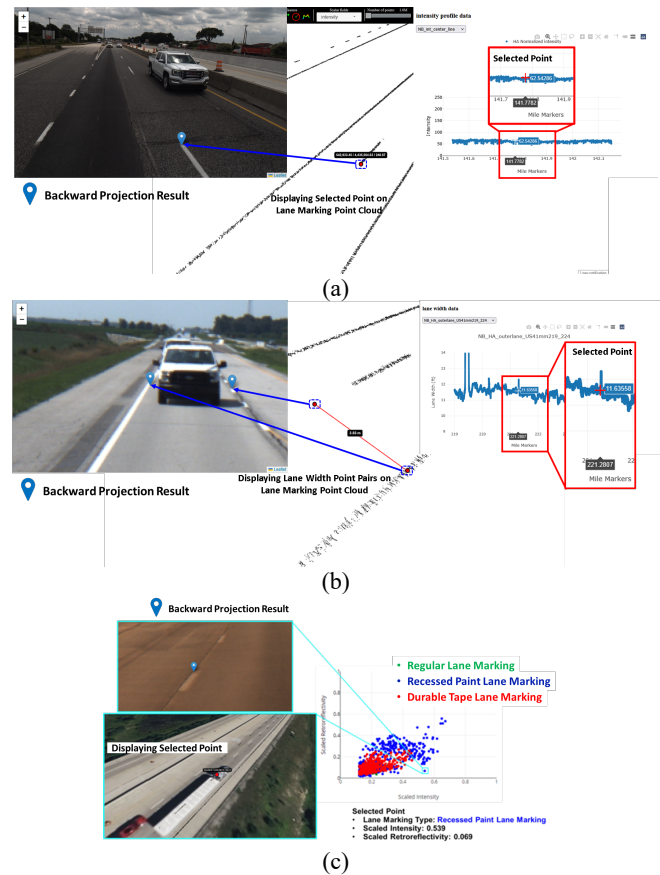


Figure 7. Illustration of web portal visualization of (a) lane marking point cloud along with its corresponding image and intensity profile, (b) lane marking point cloud along with its corresponding image and lane width profile, and (c) intensity-retroreflectivity scatter plot visualization.

3. Implementation and Validation

This section explores the capability of the web portal and its developed functionalities for quality control across various transportation corridor management scenarios. The following subsections present use cases that highlight the following web portal's major functionalities: 1) case studies that demonstrate generalized functions for evaluating the georeferencing quality of geospatial data/products, and 2) a case study utilizing the specialized functionalities for road asset management.

3.1 Case Studies that Demonstrate the Generalized Functions

3.1.1 Case Study 1: Quality Control of Multi-Modal, Multi-Platform, and Multi-Temporal Geospatial Data

Valid system calibration parameters and trajectory information are critical for generating accurately georeferenced geospatial data/products. This case study demonstrates the web portal's built-in/developed tools for evaluating georeferencing quality of transportation-related geospatial data/products. For this research objective, two wheel-based mobile mapping systems—Purdue Wheel-based Mobile Mapping System – High Accuracy (PWMMS-HA) and Purdue Wheel-based Mobile Mapping System – Ultra High Accuracy (PWMMS-UHA)—as presented in Figure 8a and Figure 8b, and a DJI M300 UAV system, as shown in Figure 8c, are employed to collect multi-modal, multi-platform, and multi-temporal geospatial data. Figure 9 shows

the study site along the I-65 highway in Indiana, USA and the description of the datasets is summarized in Table 2. The PWMMS-HA is equipped with four LiDAR units—three Velodyne HDL-32E (Velodyne, 2020a) and one Velodyne VLP-16 High-Res (Velodyne, 2020b)—and three FLIR Grasshopper3 9.1 MP GigE color cameras (Teledyne FLIR LLC, 2024b). All the sensors are georeferenced by an Applanix POS LV 220 GNSS/INS unit (Applanix, 2024). The PWMMS-UHA includes two profiling LiDAR units—a Riegl VUX 1HA (Riegl, 2020) and a Z+F Profiler 9012 (Z+F, 2020). There are also two rear-facing FLIR Flea2 FireWire color cameras (Teledyne FLIR LLC, 2024a). These LiDAR and RGB camera units are directly georeferenced by a NovAtel ProPak6 GNSS receiver (HEXAGON, 2024) and ISA-100C near-navigation grade inertial measurement unit (IMU) (NovAtel, 2022). The DJI M300 is equipped with a Zenmuse L1 LiDAR (Livox sensor), a 1-inch CMOS camera, and an IMU on a 3-axis stabilized gimbal (DJI, 2025).

Misalignments between acquired imagery and LiDAR data are usually the result of unreliable GNSS/INS trajectory and/or erroneous intrinsic/extrinsic system calibration parameters. Zhou et al. (2023) proposed the Unified Multi-Sensor Advanced Triangulation (UMSAT) algorithm to enhance the trajectory and/or system calibration parameters in such scenarios. To illustrate the impact of this enhancement, the web portal is used to visualize the data alignment quality before and after the UMSAT optimization. Specifically, to assess the georeferencing quality of multi-modal/multi-platform/multi-temporal geospatial data, the profile extraction tool from the web portal is utilized to check the alignment. Figure 10a shows the location of extracted profiles from the PWMMS-HA and DJI M300 UAV LiDAR data. The side view in Figure 10b reveals a noticeable misalignment. The UMSAT refinement results in the improvement of alignment between the two systems, as presented in Figure 10c. In addition, the backward projection function is also tested on these datasets; a selected LiDAR object point is projected onto the 2D imagery captured from all platforms, as shown in Figure 11a, using the original trajectory and system calibration parameters. From Figure 11b, one can notice that the accuracy of the backward projection improves after UMSAT.

Highway Area	Data Collection Date	Data Acquisition Platforms
I-65	July 10, 2022, and September 18, 2023	PWMMS-HA
	December 2, 2022, and September 18, 2023	PWMMS-UHA
	August 2, 2022,	DJI M300 UAV

Table 2. Description of MMS collection dates and data acquisition platforms used.



(a)



(b)



(c)

Figure 8. Illustration of data acquisition systems, showing the (a) PWMMS-HA, (b) PWMMS-UHA, and (c) DJI M300 platforms.

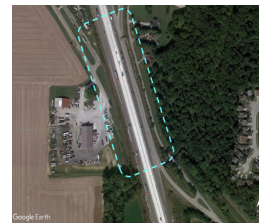
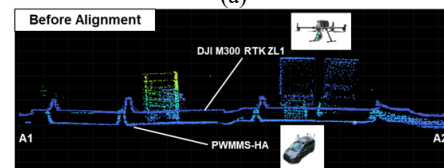


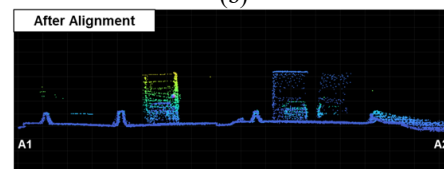
Figure 9. Illustration of the data acquisition site showing the I-65 highway with the Region of Interest (ROI) highlighted by a cyan box.



(a)

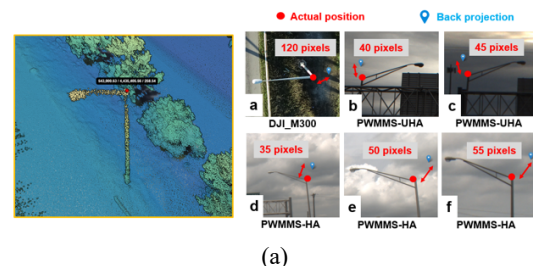


(b)



(c)

Figure 10. Illustration of (a) a profile location along the I-65 highway together with extracted profile showing the PWMMS-HA and UAV data alignment (b) before and (c) after UMSAT refinement.



(a)

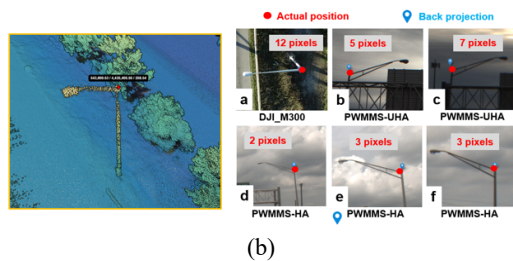


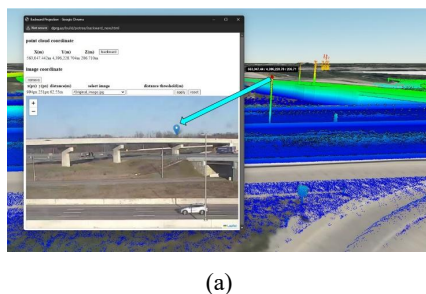
Figure 11. Illustration of a selected point on a light pole marked by a red dot that has been back projected onto imagery as a blue placeholder (a) before and (b) after UMSAT refinement.

3.1.2 Case Study 2: PTZ Camera Calibration Validation

Accurate calibration of PTZ camera systems is crucial for their precise pointing towards points of interest along the transportation corridor. However, factors such as environmental conditions, routine maintenance, and reinstallation can lead to deviations in both intrinsic and extrinsic calibration parameters, compromising the pointing accuracy to have a specific location at the center of the PTZ camera's field of view. To overcome these challenges, researchers have explored various automated calibration approaches. In this case study, the automated PTZ camera calibration approach proposed by Hany et al. (2025) is used for demonstration. When the camera is properly calibrated, the backward/forward projected points align precisely with their respective features in both 2D imagery and 3D LiDAR data. For this case study, we used forty-five PTZ cameras (AXIS, 2024) along the I-465 ring highway in Indianapolis, Indiana, USA as shown in Figure 12a and Figure 12b, respectively. The backward projection function from the web portal was utilized to validate the intrinsic/extrinsic camera calibration parameters. Figure 13 shows an example of the validation result for one camera. One can notice that the accuracy of backward projection improved after the calibration process, as presented in Figure 13b.



Figure 12. Illustration of (a) a PTZ camera and (b) the acquisition site showing the I-465 ring highway with the locations of PTZ cameras marked as red circles.



(a)

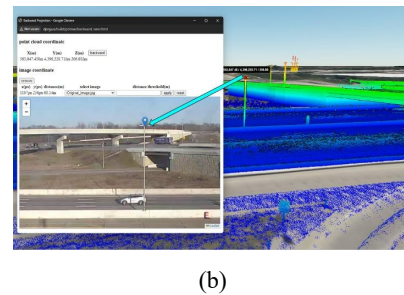


Figure 13. Illustration of backward projection result for a selected point on the light pole (a) before and (b) after PTZ camera calibration.

3.2 Case Study that Implements Specialized Functions: Lane Marking Quality Assessment

The web portal capabilities in evaluating lane marking conditions are illustrated through a case study, where two wheel-based mobile mapping systems—PWMMS-HA and PWMMS-UHA—are utilized to acquire data along the I-65 and I-74 highway in Indiana, USA as shown in Figure 14. The data collection occurred on July 7, 2022 and September 18, 2023.

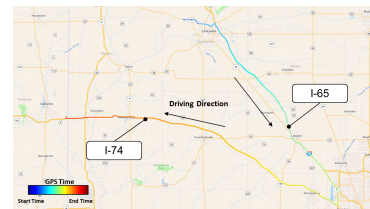


Figure 14. Illustration of the I-65 and I-74 highway showing the MMS trajectory colored by GPS time.

As demonstrated in Figure 15a, the MMS web portal features simultaneous visualization of LiDAR-derived lane marking point clouds and geo-tagged imagery. This feature facilitates direct comparison between point cloud data and RGB imagery, enhancing the interpretability of lane marking conditions. Additionally, the system supports concurrent visualization of lane marking point clouds and their associated intensity profiles. One can use this feature to assess intensity variations, which may indicate degradation in lane markings condition. For instance, Figure 15b presents a low-intensity point selected in the intensity profile and its corresponding geotagged imagery, revealing degraded lane marking. Conversely, Figure 15c displays a high-intensity point selected in the intensity profile, with its corresponding geotagged imagery indicating a freshly painted lane marking. Beyond intensity visualization, the web portal provides a tool for illustrating lane width profiles derived from lane marking point cloud data. As illustrated in Figure 15d, a point pair indicating narrow lane is mapped onto corresponding imagery. This functionality aids in detecting narrow lane locations and/or irregularities and can, therefore, serve as a tool to ensure compliance with regulatory standards.

Previous research has shown that lane markings typically have high retroreflectivity and LiDAR intensity (Zehr et al., 2019; Cheng et al., 2020; Cheng et al., 2022). Mahlberg et al. (2021) demonstrated a correlation between these two metrics, which can be used to assess lane marking quality. The web portal includes an intensity/retroreflectivity scatter plot add-on to analyze this relationship and identify anomalies in data points (for example, when a high intensity point is found to have low retroreflectivity and vice versa). Additionally, it allows users to visualize these points within the lane marking point cloud and

the corresponding imagery where they are visible. Figure 16a highlights a point in the scatter plot with high intensity and low retroreflectivity. Based on the web portal's visualization tool, this high intensity point corresponds to a freshly painted lane marking in the imagery with high intensity. The low retroreflectivity is likely due to an error in the retroreflectivity measurement. This suggests that LiDAR intensity provides a more reliable representation of the lane marking's reflective properties. Figure 16b shows a point with high retroreflectivity and low intensity. A closer inspection of the imagery at this location reveals the presence of crack sealing which is likely the cause of the high retroreflectivity. The integration of these functionalities within the web portal significantly enhances the efficiency and reliability of lane marking assessment, thereby improving the decision-making process for better management of transportation corridors.

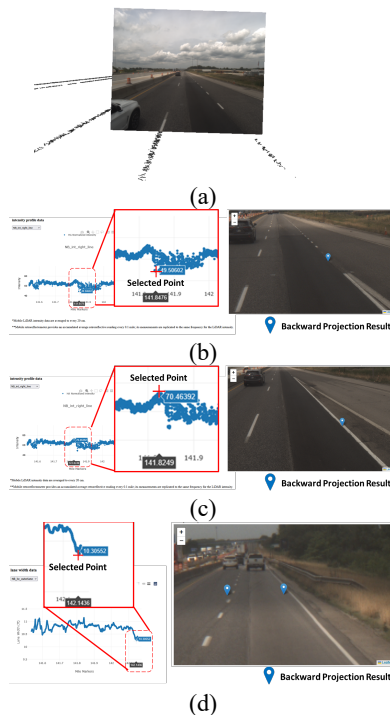


Figure 15. Illustration of lane marking quality assessment: (a) simultaneous visualization of LiDAR-derived lane marking point clouds and geo-tagged imagery, intensity profile visualization of locations with (b) high intensity, (c) low intensity, and (d) point pair in a region with narrower lane width back-projected onto the 2D imagery.

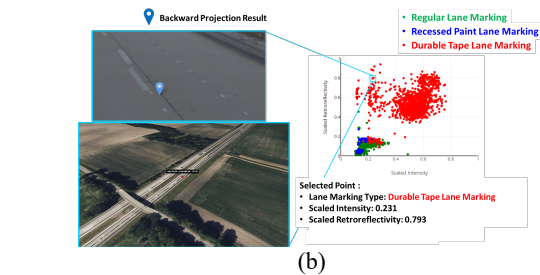
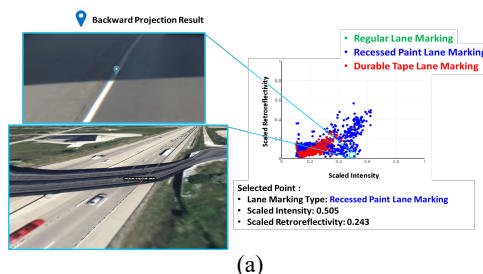


Figure 16. Illustration of intensity-retroreflectivity scatter plot visualization: (a) high intensity point corresponding to low retroreflectivity values along I-65 highway for right edge line and (b) low intensity point corresponding to high retroreflectivity values along I-74 highway for skip line.

4. Discussion and Concluding Remarks

This study presents a Potree-based web portal designed for the management, visualization, and quality control of geospatial data collected along transportation corridors. The proposed web portal provides users with tools for assessing georeferencing quality, which is necessary for reliable interpretation and decision-making using multi-modal, multi-platform, and multi-temporal geospatial data. Moreover, the developed portal and its functionalities can be used for evaluating the validity of intrinsic/extrinsic calibration of PTZ cameras that often undergo significant changes due to environmental conditions and maintenance operations. Specialized functionalities are designed for analyzing/interpreting MMS LiDAR-derived products such as pavement marking intensity and lane width. Through the few presented case studies, the web portal demonstrates its potential as a powerful tool for data-driven decision-making in transportation asset management.

Future work will focus on expanding the capabilities of the MMS web portal by incorporating additional functionalities tailored to transportation and urban planning applications. Additionally, extending the portal's application to broader use cases, such as outdoor/indoor stockpile volume estimation/monitoring, hydraulic site visualization, and urban streetscape mapping will be investigated.

Acknowledgment

This work was supported by the Joint Transportation Research Program administered by 1071 the Indiana Department of Transportation and Purdue University (grant no. SPR-1072 4742).

References

- Applanix, 2024. Applanix POS LV. <https://www.applanix.com/downloads/products/specs/POS-LV-Datasheet.pdf> (30 January 2024).
- AXIS Communications. Axis Q6075-E PTZ Network Camera, 2024. <https://www.axis.com/products/axis-q6075-e/> (7 September 2024).
- Brinster, G. L., Hodaei, M., Eissa, A. M., DeLoach, Z., Bruno, J. E., Habib, A., Bullock, D. M., 2024. Evaluating Mobile LiDAR Intensity Data for Inventorying Durable Tape Pavement Markings. *Sensors*, 24(20), 6694.
- Carey, C., Romero, J., Laefer, D. F., 2021. New Potree shader capabilities for 3D visualization of behaviors near COVID-19 rich healthcare facilities. *The International Archives of the*

Photogrammetry, Remote Sensing and Spatial Information Sciences, 46, 61-66.

Cheng, Y. T., Patel, A., Wen, C., Bullock, D., & Habib, A., 2020. Intensity thresholding and deep learning based lane marking extraction and lane width estimation from mobile light detection and ranging (LiDAR) point clouds. *Remote Sensing*, 12(9), 1379.

Cheng, Y. T., Lin, Y. C., & Habib, A., 2022. Generalized LiDAR intensity normalization and its positive impact on geometric and learning-based lane marking detection. *Remote Sensing*, 14(17), 4393

Cheng, Y. T., Shin, Y. H., Shin, S. Y., Koshan, Y., Hodaei, M., Bullock, D., & Habib, A., 2024. Image-Aided LiDAR Extraction, Classification, and Characterization of Lane Markings from Mobile Mapping Data. *Remote Sensing*, 16(10), 1668.

DJI, 2025. https://optron.com/dji/wp-content/uploads/2020/05/ds_dji-matrice-300-rtk.pdf (7 February 2025).

Girardeau-Montaut, D., 2016. CloudCompare. France: EDF R&D Telecom ParisTech, 11(5).

Habib, A., Lin, Y. J., Ravi, R., Shamseldin, T., & Elbahnasawy, M., 2018. LiDAR-based mobile mapping system for lane width estimation in work zones.

Hany, Y., Abdelghany, A. A., Eissa, A. M., Hodaei, M., Liu, J., Shin, S. Y., & Habib, A., 2025. Automated intrinsic/extrinsic PTZ camera calibration using mobile LiDAR data. *Measurement*, 117023.

Hawkins, N. R., 2013. Use of transportation asset management principles in state highway agencies (Vol. 439). Transportation Research Board.

HEXAGON, 2024. ProPak6. <https://novatel.com/support/previous-generation-products-drop-down/previous-generation-products/propak6-receiver/> (30 January 2024).

Liu, C., Song, B., Fu, M., Meng, X., Zhao, Y., Wang, X., Li, X., Liu, Z., Han, Y., 2023. Cesium-MRS: A Cesium-based Platform for Visualizing Multi-source Remote Sensing Data. *The International Archives of the Photogrammetry, Remote Sensing and Spatial Information Sciences*, 48, 15-19.

Mahlberg, J. A., Cheng, Y. T., Bullock, D. M., & Habib, A., 2021. Leveraging LiDAR intensity to evaluate roadway pavement markings. *Future transportation*, 1(3), 720-736.

Mathew, J. K., Malackowski, H. A., Gartner, C. M., Desai, J., Cox, E. D., Habib, A. F., & Bullock, D. M., 2023. Methodology for Automatically Setting Camera View to Mile Marker for Traffic Incident Management. *Journal of Transportation Technologies*, 13(4), 708-730.

NovAtel, 2022. IMU-ISA-100C technical specifications. https://docs.novatel.com/OEM7/Content/Technical_Specs_IMU/ISA_100C_Overview.html (2 September 2022).

Plas.io, 2014. <https://github.com/verma/plasio> (8 February 2025)

Ravi, R., Cheng, Y. T., Lin, Y. C., Lin, Y. J., Hasheminasab, S. M., Zhou, T., ... & Habib, A., 2019. Lane width estimation in work zones using LiDAR-based mobile mapping systems. *IEEE Transactions on Intelligent Transportation Systems*, 21(12), 5189-5212.

Riegl, 2020. Riegl VUX-1HA specification. http://www.riegl.com/uploads/tx_pxpriegldownloads/Datasheet-RIEGL_VUX-1HA_2020-08-19.pdf (19 August 2020).

Scheiblauer, C., Wimmer, M., 2011. Out-of-core selection and editing of huge point clouds. *Computers & Graphics*, 35(2), 342-351.

Schütz, M., 2015. Potree: Rendering large point clouds in web browsers (Doctoral dissertation, Technische Universität Wien).

Schütz, M., Krösl, K., Wimmer, M., 2019. Real-time continuous level of detail rendering of point clouds. In *2019 IEEE Conference on Virtual Reality and 3D User Interfaces (VR)* (pp. 103-110). IEEE.

Shen, Y., & Zhang, X., 2023. Intelligent manufacturing, green technological innovation and environmental pollution. *Journal of Innovation & Knowledge*, 8(3), 100384.

Teledyne FLIR LLC, 2024a. FireWire cameras. <https://www.flir.com/support/products/firewire-cameras/#Overview> (30 January 2024).

Teledyne FLIR LLC, 2024b. Grasshopper3 GigE. <https://www.flir.com/products/grasshopper3-gige/?vertical=machine+vision&segment=iis> (30 January 2024).

Toth, C. K., 2009. R&D of mobile LiDAR mapping and future trends. In *Proc. ASPRS Annu. Conf* (pp. 9-13).

Velodyne, 2020a. HDL32E Data Sheet. <https://velodynelidar.com/products/hdl-32e/> (19 February 2020).

Velodyne, 2020b. Puck Hi-Res Data Sheet. <https://velodynelidar.com/products/puck-hi-res/> (19 February 2020).

Yeshwanth Kumar, A., Noufia, M. A., Shahira, K. A., Ramiya, A. M., 2019. Building information modelling of a multi-storey building using terrestrial laser scanner and visualization using Potree: An open-source point cloud renderer. *The International Archives of the Photogrammetry, Remote Sensing and Spatial Information Sciences*, 42, 421-426.

Z+F, 2020. Z+F Profiler 9012 Specification. https://www.zf-laser.com/fileadmin/editor/Datenblaetter/Z_F_PROFILER_9012_Datasheet_E_final_compr.pdf (19 August 2020).

Zehr, S., Hardin, B., Lowther, H., Plattner, D., Wells, T., Habib, A., & Bullock, D. M., 2019. Rumble Stripes and Pavement Marking Delineation (No. FHWA/IN/JTRP-2019/15). United States. Department of Transportation. Intelligent Transportation Systems Joint Program Office.

Zhou, T., Liu, J., Shin, S., Habib, A., 2023. Multi-Primitive Triangulation of Airborne and Terrestrial Mobile Mapping Image and LIDAR Data. *The International Archives of the Photogrammetry, Remote Sensing and Spatial Information Sciences*, 48, 587-594.